Nanoscale

Simultaneous Detection of Multiple Proteases using a Non-array Nanopore Platform

Journal:	*Nanoscale*
Manuscript ID	NR-ART-06-2021-004085.R1
Article Type:	Paper
Date Submitted by the Author:	24-Jul-2021
Complete List of Authors:	Chen, Xiaohan; Illinois Institute of Technology, Department of Chemistry Zhang, Youwen; Illinois Institute of Technology, Department of Chemistry Guan, Xiyun; Illinois Institute of Technology, Department of Biological and Chemical Sciences

Simultaneous Detection of Multiple Proteases using a Non-array Nanopore Platform

Xiaohan Chen, Youwen Zhang, and Xiyun Guan*

Department of Chemistry, Illinois Institute of Technology, 3101 S Dearborn St., Chicago, IL 60616, USA

Supporting Information

ABSTRACT: Multiplexing methods which are capable of measurement of multiple analytes in a single assay are of great importance in many fields. The conventional strategy for simultaneous detection of multiple species is to construct a sensor array. Herein, we report an innovative multiplex multi-analyte detection platform in a non-array format for protease measurement. By monitoring protease degradation of a single peptide substrate containing two cleavage sites for a disintegrin and metalloproteinase 10 (ADAM10) and a disintegrin and metalloproteinase 10 (ADAM17) in a single nanopore, simultaneous detection and quantification of these two model proteases in mixture samples could satisfactorily be accomplished. Our developed multiplexing sensing platform has the potential to be coupled with the traditional sensor array to further improve the multiplexing capability of the sensor, which may find useful applications in clinical diagnosis and prognosis.

Key Words: Nanopore, Proteases, Simultaneous detection, Peptide substrate, Non-array format

1. Introduction

Multiplexing methods which are capable of detection & quantification of multiple analytes in a single assay are of great importance in many fields, including medical diagnosis, drug discovery, environment monitoring, and personal healthcare. Such concurrent detection techniques have many advantages over single-analyte measurement systems. These include decrease in errors between inter-sampling, reduced sample/reagent volume, improved turnaround time, and reduced assay costs. The traditional strategy for simultaneous measurement of multiple species is to construct a sensor array, in which each individual sensing probe is highly selective for a different analyte[1,2,3]. A variety of sensor array methods using different readout techniques have been developed, including colorimetry, fluorescence, electrochemistry, and so on[4,5,6]. Herein, by taking advantage of the multi-analyte detection capability of the nanopore sensor, we report an innovative multiplexing strategy for simultaneous detection of multiple proteases using a single nanopore and a single peptide substrate. Although the conventional sensor array has advantages of easy operation and simple data analysis, our developed non-array format multiplexing method may further reduce the assay cost. For proof-of-concept purpose, in this work, we use a disintegrin and metalloproteinases (ADAMs)[7] as model analyte species to demonstrate this new multiplexing nanopore-based sensing platform.

ADAMs are a family of metalloproteinases that play important roles in a variety of biological processes, including ectodomain shedding, cell surface remodeling, mediating cell-cell and cell-matrix interactions, and regulation of growth factor availability. Among the more than 30 ADAMs identified thus far, 22 are well-documented in humans. The ADAM molecule generally consists of six domains, including a metalloproteinase pro-domain, a disintegrin domain, an epidermal growth factor-like domain, a cysteine-rich domain, a transmembrane domain and a cytoplasmic domain[8]. Numerous studies (using cell lines, animal models and human malignancies) have shown that ADAMs are implicated in various diseases such as Rheumatoid arthritis, Alzheimer's disease, cardiac hypertrophy, asthma, and cancer, and hence have become novel biomarkers and potential therapeutic targets for disease early detection and treatment[9,10]. For example, the overexpression of ADAM12 is conducive to tumor growth and progression in breast and prostate cancers

through decreasing apoptosis of tumor cells[11], while an up-regulated level of ADAM15 contributes to cancer progression by shedding cadherin E to activate HER2/HER3[12]. It was also found out that ADAM10 and ADAM17 could mediate HER/EGFR ligands, thus affecting cell proliferation, migration, and survival [13].

The use of nanopores as a versatile tool for exploring various applications at the single molecule level has received increased attention during the past decade [14,15,16]. Several examples of nanopore applications include DNA sequencing, environmental monitoring, disease detection, and cellular metabolism study[17,18,19,20]. In nanopore sensing, analyte molecules are driven through a nanochannel (biological protein or synthetic nanopore) [21,22,23,24,25,26] via electrophoretic effect and/or diffusion force under an applied potential bias, producing transient ionic current modulations (events)[27]. The event signatures such as frequency, blockage amplitude, and residence time can be utilized to reveal the concentration and the identity of the analyte[28]. In our previous study, we pioneered a label-free real-time method to monitor peptide-protease cleavage interaction using a protein nanopore by taking advantage of the significantly different event residence time and/or amplitude values of the peptide substrate and its breakdown products due to their length difference[29]. This method was further advanced to measure protease activity [30,31,32]. In this work, we develop a multiplexing technique to simultaneously detect multiple proteases using a single nanopore and a single peptide substrate.

2. Material and methods

2.1. Materials and reagents

Peptide substrate for ADAM10 and ADAM17 (sequence: RLAQAVRSSSARLVFFKPLGLARL) and its cleavage fragments (sequences: ARL, RSSSARLVFFKPLGL, and RLAQAVRSSSARLVFFKPLGL) were synthesized by WatsonBio (Houston, TX). Both ADAM10 and ADAM17 were ordered from R&D Systems (Minneapolis, MN). 1,2-diphytanoylphosphatidylcholine was obtained from Avanti Polar Lipids (Alabaster, AL). Other chemicals, including sodium chloride, zinc chloride, Trizma base, hydrochloric acid, pentane, hexadecane, HPLC-grade water, and DNase, RNase free water, were purchased from Sigma-Aldrich (St. Louis, MO). The stock solutions of ADAM10 and ADAM17 were prepared in DNase, RNase free water at a concentration of 100 μg/mL and 10 μg/mL, respectively, and stored at -80 °C before and immediately after use. The stock solutions of peptides (5 mM each) were also prepared with DNase, RNase free water and kept at -20 °C before and immediately after use.

2.2. Preparation and formation of protein pore

The preparation of protein nanopores has been described in our previous work[33]. Briefly, the wild-type (WT) α-hemolysin (αHL) protein monomers were first synthesized by coupled *in vitro* transcription and translation (IVTT) using the *E. Coli* T7 S30 Extract System for Circular DNA from Promega (Madison, WI) and with a WT αHL gene [34] in a T7 vector (pT7–αHL). After addition of rabbit red cell membranes and incubating for 1 h, they were assembled into homoheptamers [35]. The heptamers were then purified by SDS-polyacrylamide gel electrophoresis and stored in aliquots at -80°C.

2.3. Bilayer Experiment and Data Analysis

The detailed procedures regarding nanopore electrical recordings have been described previously[33]. Briefly, a planar lipid bilayer of 1, 2-diphytanoylphosphatidylcholine was formed according to Montal-Mueller method [34] on a 100-μm aperture of a PTFE film (Goodfellow, PA) which was anchored between two chamber compartments (*cis* and *trans*). Unless otherwise noted, the experiments were performed at 24 ± 1 °C with the WT αHL protein and the peptide / peptide cleavage products added to the *cis* and *trans* chamber compartments, respectively.

2.4. Enzyme Digestion

Enzymatic reactions were carried out in 40-μL mixtures, containing ADAM10/ADAM17 (with concentrations ranging from 25 to 200 ng/mL), 5 μL of $ZnCl_2$ buffer solution (consisting of 5 μM $ZnCl_2$, 0.15 M NaCl, and 50 mM Tris, pH 7.5), and 1 μL of 5 mM peptide substrate. The mixtures were incubated at 37 °C for 60 min. All the digestion products were stored at -20 °C before nanopore analysis.

3. Results and discussions

3.1. Principle of Simultaneous Detection of Multiple Proteases in a Nanopore and Substrate Peptide Design

Unlike the conventional sensor array, in our developed multiplexing strategy, simultaneous detection of multiple proteases was carried out by monitoring the translocation of a single peptide substrate in a single nanopore where the substrate contained multiple cleavage sites for multiple proteases. As a proof-of-concept purpose, the principle for concurrent detection of two proteases (i.e., ADAM10 and ADAM17) was shown in Scheme 1. If the sample only contains ADAM10, the peptide substrate will be degraded into two fragments, thus producing one or two types of new events (depending on the nanopore resolution and the length/sequence difference between the produced two fragments). In contrast, if the sample only contains ADAM17, it would cleave the substrate and produce another pair of fragments. Since the substrate breakdown products by ADAM17 are different from those of ADAM10, they would produce events with different signatures, thus allowing ADAM10 and ADAM17 to be differentiated. On the other hand, if both ADAM10 and ADAM17 are present in the sample solution, the two representative events (attributed to the ADAM10 or ADAM17 cleavage products) discussed in the above two cases would be observed. In addition, it is likely that the same peptide substrate will be cleaved by both the proteases simultaneously or sequentially, so that three peptide fragments will be produced, leading to generation of other types of new events.

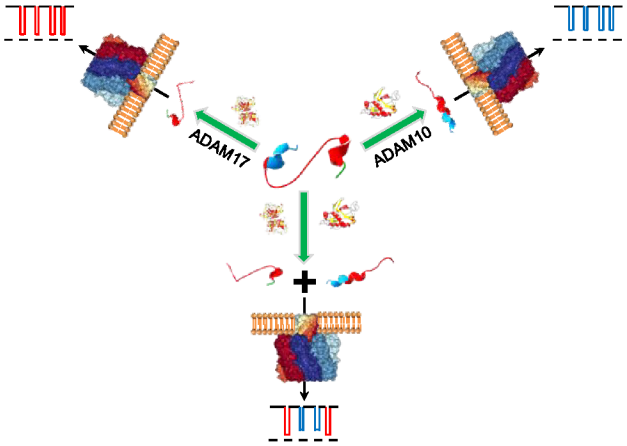

Scheme 1. Schematic representation of the principle for simultaneous detection of ADAM10 and ADAM17 using a single nanopore and a single substrate.

In our study, a 24-mer peptide with a sequence of RLAQAVRSSSARLVFFKPLGLARL was utilized as the substrate for the concurrent detection of ADAM10 and ADAM17. Note that this peptide was designed so that it contained three critical segments. Among them, KPLGL-AR and LAQAV-RSSSAR were well-documented substrates for ADAM10 and ADAM17, respectively, where the cleavage sites were indicated by the hyphens [38,39]. The reason why a peptide segment of LVFF was inserted between the two substrate sequences is because it could significantly improve the residence time and frequency of the peptide events, which has been documented in our previous studies[32,40]. To facilitate differentiation between substrate degradation products by ADAM10 and ADAM17, an arginine and a leucine were additionally added. With such a peptide substrate, a 3 amino acid (AA) fragment and a 21 AA fragment would be produced if the sample contains ADAM10, while a 6 AA fragment and an 18 AA fragment would be produced if there is presence of ADAM17 in the solution. If the sample is consisted of both ADAM10 and ADAM17 and if the substrate can be cleaved by both the proteases, three fragments (3 AA, 6

AA, and 15 AA) could be generated. However, in our designed substrate sequence, the space between the two cleavage sites is ~ 5-6 nm (15 AA), while the dimensions of ADAM10 and ADAM17 are both larger than 7 nm [41,42]. Therefore, the chance for simultaneous degradation of the substrate by both proteases would be low although we could not rule out the possibility of sequential digestion of the substrate by ADAM10 and ADAM17. It should be noted that, due to the low resolution of the wild-type α-hemolysin pore, short peptides such as the 3-mer and 6-mer fragments in our study rarely produce observable current modulation events due to their weak interaction with the protein pore (note that a control experiment with a synthesized 3-mer peptide in the nanopore was provided in Supporting Information, Fig. S1). Accordingly, at most 3 types of fragment events (corresponding to 15 AA, 18 AA, and 21 AA) could be expected.

3.2. Optimization of Experimental Conditions

Electrolyte effect on nanopore sensitivity and resolution. Initial experiments were performed at +120 mV under symmetric electrolyte conditions with both the *cis* and *trans* chamber compartments filled with 1 M NaCl buffer solutions (pH 7.5). To evaluate whether the designed peptide sequence could enable nanopore differentiation among the peptide substrate and its ADAM10 / ADAM17 cleavage products, three samples (i.e., the substrate alone, the incubation mixture of the substrate and ADAM10, and the reaction mixture of the peptide substrate and ADAM17) were examined. The experimental results were summarized in Fig. 1. We could see that although the events of the three samples were significantly overlapped, they did show different signatures. For example, the substrate events had a mean residual current of 22.7 ± 0.7 % of full channel block, while the substrate / ADAM10 and substrate / ADAM17 mixture samples produced events with residual currents of 26.6 ± 0.3 % and 28.7 ± 0.2 % of full channel block, respectively. On the other hand, the mean residence time of the substrate events was 5.0 ± 0.4 ms, while those of the substrate / ADAM10 and substrate / ADAM17 mixtures were 4.3 ± 1.1 ms, and 2.6 ± 0.2 ms, respectively.

In order to enhance the resolution and performance of the nanopore sensor for the simultaneous detection and quantification of the substrate and its protease cleavage fragments, nanopore analysis of the three samples were further carried out under symmetric electrolyte conditions with both the *cis* and *trans* chamber compartments filled with 3 M NaCl buffer solutions (pH 7.5) and under asymmetric electrolyte conditions with the *cis* chamber compartment filled with 3 M NaCl buffer solution (pH 7.5) while with the *trans* compartment filled with 0.5 M NaCl buffer solution (pH 7.5). Note that use of a salt gradient instead of the conventional symmetric electrolyte solution and increasing the electrolyte concentration are two well-established approaches to significantly increase the event frequency and/or residence time for translocation of biomolecules through a nanopore [43,44]. As we expected, the resolution of the nanopore sensor under these two experimental conditions was indeed much improved over that in 1 M NaCl solution. To be more specific, in 3 M NaCl, the substrate peptide produced only one major type of events with a mean residual current of 9.9 ± 0.6 % of full channel block and residence time of 221.6 ± 47.3 ms. In contrast, in addition to the substrate events, the substrate / ADAM17 mixture produced a new type of events (residual current: 18.5 ± 1.3 % of full channel block; residence time: 74.2 ± 4.1 ms), while two new types of events (residual current: 18.4 ± 0.9 % channel block, residence time: 71.0 ± 7.7 ms; and residual current: 23.3 ± 0.6 % channel block, residence time: 29.2 ± 1.5 ms) were observed when the substrate / ADAM10 mixture was added to the nanopore. Clearly, the substrate and its ADAM10 or ADAM17 cleavage product events could be well separated. However, since the events of the substrate / ADAM10 mixture and the substrate / ADAM17 mixture were significantly overlapped, simultaneous quantification of ADAM10 and ADAM17 in 3 M NaCl was difficult if not impossible. In the case of analyzing the three samples under a salt gradient, we found that the peptide substrate

and its ADAM10/ADAM17 digestion products produced significantly different events (residual current: 19.6 ± 0.9 % channel block, residence time: 22.9 ± 2.4 ms; residual current: 31.2 ± 0.4 % channel block, residence time: 7.6 ± 1.2 ms; and residual current: 25.3 ± 0.5 % channel block, residence time: 14.2 ± 1.8 ms, respectively). Although the events of the substrate and its ADAM17 digestion products were overlapped to some extent if only the block amplitude was considered, combined use of the event residence time and amplitude enabled their differentiation and simultaneous quantification (Supporting Information, Fig. S2). Taken together, the combined results suggested that, among the three experimental conditions, nanopore detection of peptides achieved the highest sensitivity in a salt gradient, in which the event frequency of, e.g., the substrate was ~10.2 folds and ~17.2 folds larger than that in 1 M NaCl and 3 M NaCl symmetric buffer conditions, respectively. In contrast, 3 M NaCl solution offered the nanopore sensor the best resolution (e.g., the substrate τ_{off} value was ~44.3 / ~9.7 folds larger than that in 1 M NaCl symmetric and salt gradient electrolyte solutions, respectively). Since the events of the substrate cleavage products by ADAM10 and ADAM17 in 3 M NaCl were significantly overlapped, 3 M (*cis*) / 0.5 M (*trans*) NaCl asymmetric buffer condition was deemed as the optimal buffer solution for simultaneous detection of ADAM10 and ADAM17, and used in the remaining experiments. In addition, we noticed that the events of the substrate peptide degradation fragment by ADAM10 (i.e., peptide RLAQAVRSSSARLVFFKPLGL) and those of the synthesized peptide standard had different blockage amplitude values (~31% vs. ~24%, Figs. 1 and S1), which might be attributed to the difference in their structures.

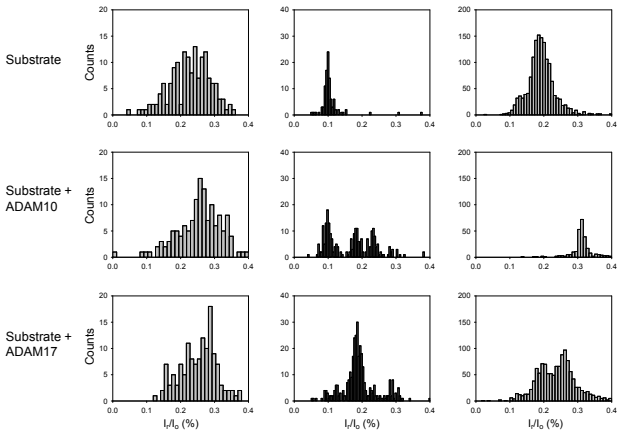

Figure 1. Amplitude histograms, showing the salt effect on nanopore detection and differentiation of the substrate peptide and its enzymatic cleavage products. (*Left*) 1 M (*cis*) / 1 M (*trans*) NaCl; (*middle*) 3 M (*cis*) / 3 M (*trans*) NaCl; and (*right*) 3 M (*cis*) / 0.5 M (*trans*) NaCl. The experiments were performed at +120 mV with the wild type α-hemolysin protein nanopore. The concentration of the peptide substrate used was 2.5 μM, while those of ADAM10 and ADAM17 were 200 ng/mL and 75 ng/mL, respectively.

Effect of the applied potential on nanopore detection of ADAM10 and ADAM17. To achieve the maximum nanopore performance for the highly sensitive detection of ADM10 and ADAM17, the effect of the applied voltage bias on the translocation of the peptide substrate and its ADAM10/ADAM17 degradation products in the nanopore was further investigated. The plots of the event frequency, residual current, and the mean residence time as a function of the voltage (ranging from +40 mV to +120 mV) were summarized in Fig. 2. We could see that, with an increase in the applied potential bias, the event frequencies for all the three samples increased. For example, between +40 mV and +120 mV, their event frequencies increased ~8.6 folds, ~2.8 folds, and ~4.0 folds, respectively. Unlike the event frequencies which are voltage dependent, the event blockage amplitudes (normalized residual currents) for all the three samples didn't change significantly with the voltage. On the other hand, as the voltage increased, the event mean residence

time values for the peptide substrate and its protease cleavage products first increased and then decreased, suggesting that the residence time of the peptides in the protein pore has a biphasic voltage dependence, which is in agreement with the previous report [45]. Since the peptide events had relatively large values for all the three parameters (frequency, residence time, and blockage amplitude) at +120 mV, this voltage was deemed as the optimum potential bias and used in the remaining experiments.

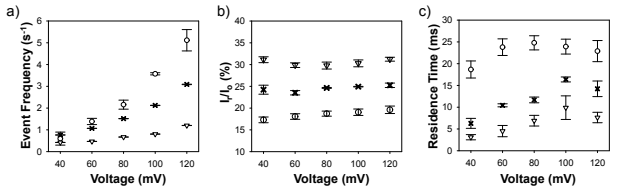

Figure 2. Effect of the applied voltage bias on peptide translocation in the nanopore: (○) substrate only; (▽) substrate + ADAM10; and (×) substrate + ADAM17. The experiments were performed under asymmetric electrolyte conditions of 3 M (*cis*) / 0.5 M (*trans*) NaCl. The concentration of the peptide substrate used was 2.5 μM, while those of ADAM10 and ADAM17 were 200 ng/mL and 150 ng/mL, respectively.

Feasibility study for nanopore analysis of a mixture sample. To demonstrate that our nanopore sensor has the capability to simultaneously detect multiple proteases, a mixture sample was prepared by adding ADAM10 (200 ng/mL) and ADAM17 (75 ng/mL) to 2.5 μM of the peptide substrate solution. The mixture was incubated at 37 °C for 60 min, and then analyzed by the nanopore at +120 mV under a salt gradient of 3 M (*cis*) / 0.5 M (*trans*) NaCl. Our experimental results (Fig. 3) demonstrated that the mixture sample produced two types of events (residual current: 25.8 ± 0.4 % channel block, residence time: 12.3 ± 0.9 ms; and residual current: 31.4 ± 1.3 % channel block, residence time 7.1 ± 0.5 ms). These event signatures were similar to those (residual current: 25.3 ± 0.5 % channel block, residence time: 14.2 ± 1.8 ms; and residual current: 31.2 ± 0.4 % channel block, residence time: 7.6 ± 1.2 ms, respectively) of the substrate cleavage products by individual ADAM10/ADAM17 proteases. Substrate peptide events were hardly observed in the current trace of the mixture sample (Fig. 3b), indicating the enzymatic reaction was complete under our experimental condition. It should be noted that, in principle, the peptide substrate has the possibility to be simultaneously cleaved by both ADAM10 and ADAM17, thus producing three fragments (3 AA, 6 AA, and 15 AA). If that is the case, the 15 AA peptide fragment should produce a type of events with a residual current of 34.3 ± 0.1 % channel block and having a mean residence time of 3.7 ± 0.2 ms (see Supporting Information, Fig. S3). However, these events were not clearly observed, thus not supporting the hypothesis of simultaneous cleavage of the same peptide substrate by both ADAM10 and ADAM17. One likely interpretation is that the two cleavage sites in the substrate were too close to each other, thus not permitting the two proteases to access the two cleavage sites at the same time. Our experimental results also suggested that ADAM10 and ADAM17 preferred to cleave free peptides rather than sequential digestion of the substrates. On the other hand, we found that, with an increase in the length of the peptide, the normalized residual current of its events decreased (Supporting Information, Fig. S4). Therefore, it is feasible to design a new peptide substrate with two cleavage sites separated far apart to allow simultaneous cleavage between the substrate and two proteases. This study is currently underway. Taken together, our experimental results suggested that our developed nanopore sensor has the capability to simultaneously detect ADAM10 and ADAM17.

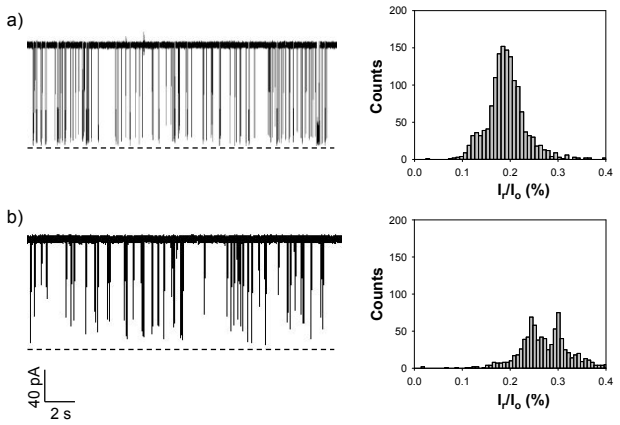

Figure 3. (*Left*) Typical trace segments and (*right*) their corresponding amplitude histograms of peptide substrate (2.5 μM) in the α-hemolysin protein nanopore in the (a) absence and (b) presence of a mixture of ADAM10 (200 ng/mL) and ADAM17 (75 ng/mL). The experiments were performed at +120 mV under asymmetric electrolyte conditions of 3 M (*cis*) / 0.5 M (*trans*) NaCl. The enzymatic reactions were incubated at 37 ˚C for 1 h.

3.3. Dose Response Curves of ADAM10 and ADAM17

To determine the sensor sensitivity, calibration curves for ADAM10 and ADAM17 were constructed, respectively, by monitoring the substrate-ADAM10 / substrate-ADAM17 cleavage interactions at +120 mV in a nanopore under a salt gradient of 3 M (*cis*) / 0.5 M (*trans*) NaCl, where the concentration of the peptide substrate was kept constant at 2.5 μM, while the concentrations of ADAM10 and ADAM17 varied from 50 ng/mL to 200 ng/mL and from 25 ng/mL to 100 ng/mL, respectively. Our experimental results (Fig. 4) showed that, with an increase in the enzyme concentration, the frequency of the produced peptide fragment events increased. It was found that the limits of detection (LODs) for ADAM10 and ADAM17 were 23.0 ng/mL and 1.5 ng/mL, respectively. Note that LOD was defined as the concentration of the enzyme corresponding to three times the standard deviation of the blank signal. It was worth mentioning that, to simply data analysis for calculating the frequency of the events attributed to the degradation of the substrate by ADAM17, all the events with residual currents of more than 22% of full channel block were included, some of which may belong to the substrate. That is the reason why the dose response curve for ADAM17 had a larger background than that for ADAM10.

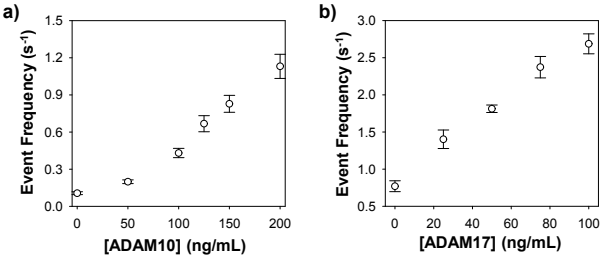

Figure 4. Plot of event frequency as a function of (a) ADAM17 and (b) ADAM10 concentration. The experiments were performed at +120 mV in a salt gradient of 3 M (*cis*) / 0.5 M (*trans*) NaCl and in the presence of 2.5 μM peptide substrate.

3.4. Analysis of ADAM10 /ADAM17 Mixture Samples

To demonstrate the potential application of our nanopore sensor in analysis of ADAM10 and ADAM17, a series of ADAM10 and ADAM17 mixture samples was prepared. For proof-of-concept purpose, and also to simply data analysis, the concentrations of ADAM10 in the mixtures were kept constant at 175 ng/mL, while those of ADAM17 varied (ranging from 25 ng/mL to 100 ng/mL). These mixture samples were analyzed with our nanopore sensor after incubating with 2.5 μM of the substrate peptide. Clearly, only the substrate events were observed for the control sample which did not contain ADAM10 or ADAM17 (Fig. 5a). However, if ADAM10 was present in the solution, a new type of events with a mean residual current of ~30% channel block appeared (Fig. 5b). Furthermore, if the sample also contained ADAM17, another type of events with a residual current of ~25% channel block could be identified (Fig. 5c). Moreover, with an increase in the concentration of ADAM17 in the mixture, the number of the events attributed to the substrate/ADAM17 cleavage fragments increased, while that of the substrate degradation products by ADAM10 did

not change significantly (Figs. 5d and 5e). To obtain the concentration of ADAM10, all the events with residual currents ranging from 28%-34% of full channel block were collected. As to ADAM17, the events with residual currents ranging from 23%-28% were used to calculate its event frequency. However, since the events of ADAM10 and ADAM17 were slightly overlapped, to mitigate the ADAM10 effect, a modified calibration curve (Supporting Information Fig. S5) was used to calculate ADAM17 concentration. Our experimental results (Table 1) showed that these ADAM10/ADAM17 mixture samples could successfully be quantitated.

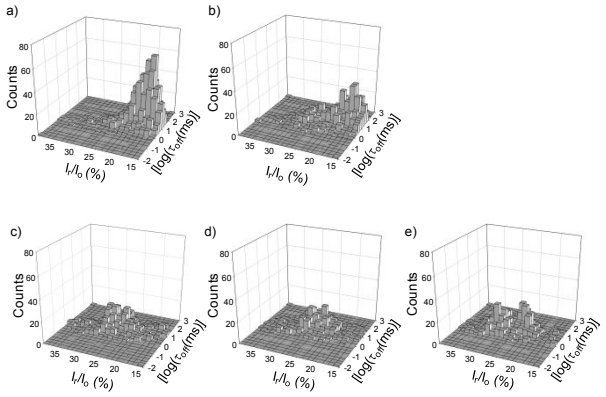

Figure 5. 3D plots of event counts vs. blockage amplitude vs. residence time, showing the simultaneous detection of ADAM10 and ADAM17. a) Substrate only (2.5 μM); b) substrate (2.5 μM) + ADAM10 (175 ng/mL); c) substrate (2.5 μM) + ADAM10 (175 ng/mL) + ADAM17 (25 ng/mL); d) substrate (2.5 μM) + ADAM10 (175 ng/mL) + ADAM17 (50 ng/mL); and e) substrate (2.5 μM) + ADAM10 (175 ng/mL) + ADAM17 (100 ng/mL). The experiments were performed at +120 mV in a salt gradient of 3 M (*cis*) / 0.5 M (*trans*) NaCl. Enlarged views of Figs. 5c-5e were displayed in Supporting Information, Fig. S6.

Table 1. Recovery of ADAM10 and ADAM17 from the mixture sample by use of our developed multiplexing nanopore sensor. Each value represents the mean of three replicate analyses ± one standard deviation.

Sample	ADAM10 (ng/L)		ADAM17 (ng/mL)	
	Theoretic Value	Experimental Value	Theoretic Value	Experimental Value
1	175	162.8 ± 38.7	25	28.9 ± 5.4
2	175	151.2 ± 26.7	50	56.2 ± 7.9
3	175	161.6 ± 33.9	100	88.2 ± 13.6

4. Conclusion

In summary, by using a single nanopore and a single peptide substrate containing two cleavage sites, we developed a novel multiplexing nanopore sensor for concurrent detection of ADAM10 and ADAM17 in a non-array format. One potential issue in the analysis of real-world (e.g., serum) samples by our developed multiplexing nanopore sensor is the matrix effect. A misconception is that the matrix components (e.g., DNA/RNA, peptides, and proteins) in these samples might block the nanopore, thus producing non-specific current modulations, which might interfere with the target analyte detection. However, it is worth mentioning that in our sensor design, detection of the target protease is achieved based on the substate peptide degradation products, or more accurately the frequencies of their events. Even if these events and those of the sample matrix components had similar blockage amplitudes and residence time values, and hence could not be well separated, we could still accurately obtain the event frequency due to the target peptide fragments by subtracting the event frequency derived in the absence of the substrate from that obtained in the presence of the substrate. Therefore, the existence of matrix components in real-world samples would not interfere with our measurement of protease activity. Furthermore, although the entire investigation in this work was focused on detection of two protease species, it could be visualized that our strategy could be applicable to other multiple protease systems as long as the nanopore sensor can provide enough resolution. Moreover, it should be noted that, the performance of the nanopore sensor could be significantly improved by utilizing engineered nanopores with appropriately introduced surface functions, as documented in our previous studies [46,47]. Alternatively, the peptide substrate needs to be carefully designed so that the

substrate cleavage fragments could produce current modulation events with well distinguishable signatures. In addition, our developed multiplexing sensing strategy could be coupled with the conventional sensor array[48] to further improve the multiplexing capability of the nanopore sensor, which may find useful applications in clinical diagnosis and prognosis.

Supporting Information

The Supporting Information is available free of charge on the Publications website.

Additional figures, including amplitude histograms of peptides ARL and RLAQAVRSSSARLVFFKPLGL, amplitude histogram of peptide RSSSARLVFFKPLGL, effect of the peptide length on the mean residual current of peptide translocation events, plot of event frequency as a function of ADAM17 concentration, and 3D plots of event counts vs. blockage amplitude vs. residence time, showing the simultaneous detection of ADAM10 and ADAM17.

Declaration of Competing Interest

The authors declare no competing financial interests.

ACKNOWLEDGMENTS

We gratefully thank National Institutes of Health (2R15GM110632-02), National Science Foundation (1708596) for supporting this work.

Notes and references

1 T. A. Taton, *Science*, 2000, **289**, 1757–1760.

2 S. Sun, K. Jiang, S. Qian, Y. Wang and H. Lin, *Anal. Chem.*, 2017, **89**, 5542–5548.

3 X. Yang, K. Qiao, F. Liu, X. Wu, M. Yang, J. Li, H. Gao, S. Zhang, W. zhou and R. Lu, *Talanta*, 2017, **166**, 93–100.

4 N. Wu, Y.-T. Wang, X.-Y. Wang, F.-N. Guo, H. Wen, T. Yang and J.-H. Wang, *Anal. Chim. Acta*, 2019, **1091**, 69–75.

5 Y. Zhang, X. Chen, G. M. Roozbahani and X. Guan, *Anal Bioanal Chem*, 2018, **410**, 6177–6185.

6 Y. Luo, Y. Wang, H. Yan, Y. Wu, C. Zhu, D. Du and Y. Lin, *Anal. Chim. Acta*, 2018, **1042**, 44–51.

7 N. Ito, S. Nomura, A. Iwase, T. Ito, F. Kikkawa, M. Tsujimoto, S. Ishiura and S. Mizutani, *Biochemical and Biophysical Research Communications*, 2004, **314**, 1008–1013.

8 A. Aljohmani and D. Yildiz, *Front Cardiovasc Med*, 2020, **7**, 608281.

9 T. Klein and R. Bischoff, *J. Proteome Res.*, 2011, **10**, 17–33.

10 M. J. Duffy, E. McKiernan, N. O'Donovan and P. M. McGowan, *Clin. Chim. Acta*, 2009, **403**, 31–36.

11 M. Kveiborg, C. Fröhlich, R. Albrechtsen, V. Tischler, N. Dietrich, P. Holck, P. Kronqvist, F. Rank, A. M. Mercurio and U. M. Wewer, *Cancer Res*, 2005, **65**, 4754–4761.

12 A. J. Najy, K. C. Day and M. L. Day, *J. Biol. Chem.*, 2008, **283**, 18393–18401.

13 M. J. Duffy, M. Mullooly, N. O'Donovan, S. Sukor, J. Crown, A. Pierce and P. M. McGowan, *Clin Proteomics*, 2011, **8**, 9.

14 D. V. Verschueren, S. Pud, X. Shi, L. De Angelis, L. Kuipers and C. Dekker, *ACS Nano*, 2019, **13**, 61–70.

15 D. Garoli, H. Yamazaki, N. Maccaferri and M. Wanunu, *Nano Lett.*, 2019, **19**, 7553–7562.

16 B. I. Karawdeniya, Y. M. N. D. Y. Bandara, J. W. Nichols, R. B. Chevalier and J. R. Dwyer, *Nat Commun*, 2018, **9**, 3278.

17 H. Bayley, *Nat Nanotechnol*, 2017, **12**, 1116–1117.

18 G. M. Roozbahani, X. Chen, Y. Zhang, R. Xie, R. Ma, D. Li, H. Li and X. Guan, *ACS Sens*, 2017, **2**, 703–709.

19 Y. Wang, D. Zheng, Q. Tan, M. X. Wang and L.-Q. Gu, *Nat Nanotechnol*, 2011, **6**, 668–674.

20 Y.-L. Ying, Y.-X. Hu, R. Gao, R.-J. Yu, Z. Gu, L. P. Lee and Y.-T. Long, *J. Am. Chem. Soc.*, 2018, **140**, 5385–5392.

21 Y.-Q. Wang, M.-Y. Li, H. Qiu, C. Cao, M.-B. Wang, X.-Y. Wu, J. Huang, Y.-L. Ying and Y.-T. Long, *Anal Chem*, 2018, **90**, 7790–7794.

22 Z. Ji, X. Kang, S. Wang and P. Guo, *Biomaterials*, 2018,

182, 227–233.

23 S. J. Fleming, B. Lu and J. A. Golovchenko, *Biophys J*, 2017, **112**, 368–375.

24 D. V. Verschueren, W. Yang and C. Dekker, *Nanotechnology*, 2018, **29**, 145302.

25 S. Banerjee, J. Wilson, J. Shim, M. Shankla, E. A. Corbin, A. Aksimentiev and R. Bashir, *Adv Funct Mater*, 2015, **25**, 936–946.

26 J. Larkin, R. Henley, D. C. Bell, T. Cohen-Karni, J. K. Rosenstein and M. Wanunu, *ACS Nano*, 2013, **7**, 10121–10128.

27 Y. Wang, Y. Zhang, X. Chen, X. Guan and L. Wang, *Talanta*, 2021, **223**, 121684.

28 G. Wang, L. Wang, Y. Han, S. Zhou and X. Guan, *Acc. Chem. Res.*, 2013, **46**, 2867–2877.

29 Q. Zhao, R. S. S. de Zoysa, D. Wang, D. A. Jayawardhana and X. Guan, *J. Am. Chem. Soc.*, 2009, **131**, 6324–6325.

30 M. Li, A. Rauf, Y. Guo and X. Kang, *ACS Sens*, DOI:10.1021/acssensors.9b01783.

31 L. Wang, Y. Han, S. Zhou and X. Guan, *Biosens Bioelectron*, 2014, **62**, 158–162.

32 S. Zhou, L. Wang, X. Chen and X. Guan, *ACS Sens*, 2016, **1**, 607–613.

33 Q. Zhao, D. A. Jayawardhana and X. Guan, *Biophys. J,*. 2008, **94**, 1267-1275.

34 L. Song, M. R. Hobaugh, C. Shustak, S. Cheley, H. Bayley and J. E. Gouaux, *Science,* 1996, **274**, 1859-1866.

35 S. Cheley, O. Braha, X. Lu, S. Conlan and H. Bayley, *Protein Sci.,* 1999, **8**, 1257-1267.

36 X. Chen, L. Wang, G. M. Roozbahani, Y. Zhang, J. Xiang and X. Guan, *Electrophoresis*, 2018, **39**, 2410–2416.

37 M. Montal and P. Mueller, *Proc. Natl. Acad. Sci. U.S.A.*, 1972, **69**, 3561–3566.

38 Y. Zhang, X. Chen, G. M. Roozbahani and X. Guan, *Analyst*, 2019, **144**, 1825–1830.

39 J. B. Schaal, T. Maretzky, D. Q. Tran, P. A. Tran, P. Tongaonkar, C. P. Blobel, A. J. Ouellette and M. E. Selsted, *J. Biol. Chem.*, 2018, **293**, 2725–2734.

40 X. Chen, Y. Zhang, G. Mohammadi Roozbahani and X. Guan, *ACS Appl. Bio Mater.*, 2019, **2**, 504–509.

41 T. C. M. Seegar, L. B. Killingsworth, N. Saha, P. A. Meyer, D. Patra, B. Zimmerman, P. W. Janes, E. Rubinstein, D. B. Nikolov, G. Skiniotis, A. C. Kruse and S. C. Blacklow, *Cell*, 2017, **171**, 1638-1648.e7.

42 Z. Guo, P. Orth, S.-C. Wong, B. J. Lavey, N.-Y. Shih, X. Niu, D. J. Lundell, V. Madison and J. A. Kozlowski, *Bioorg Med Chem Lett*, 2009, **19**, 54–57.

43 J. Ivica, P. T. F. Williamson and M. R. R. de Planque, *Anal. Chem.*, 2017, **89**, 8822–8829.

44 Y. Lin, Y.-L. Ying, X. Shi, S.-C. Liu and Y.-T. Long, *Chem Commun (Camb)*, 2017, **53**, 11564–11567.

45 L. Movileanu, J. P. Schmittschmitt, J. M. Scholtz and H. Bayley, *Biophys. J.*, 2005, **89**, 1030–1045.

46 Y. Zhang, X. Chen, C. Wang, G. M. Roozbahani, H.-C. Chang and X. Guan, *Biosens Bioelectron*, 2020, **165**, 112289.

47 Q. Zhao, D. A. Jayawardhana, D. Wang and X. Guan, *J Phys Chem B*, 2009, **113**, 3572–3578.

48 Q. Zhao, D. Wang, D. A. Jayawardhana and X. Guan, *Nanotechnology*, 2008, **19**, 505504.